PERGAMON

Vision Research 42 (2002) 19–27

Vision Research

www.elsevier.com/locate/visres

Relative contributions of bipolar cell and amacrine cell inputs to light responses of ON, OFF and ON–OFF retinal ganglion cells

Ji-Jie Pang, Fan Gao, Samuel M. Wu *

Cullen Eye Institute, Baylor College of Medicine, One Baylor Plaza, NC-205, Houston, TX 77030, USA

Received 10 July 2001; received in revised form 6 September 2001

Abstract

Light-evoked postsynaptic currents (lePSCs) were recorded from ON, OFF and ON–OFF ganglion cells in dark-adapted salamander retinal slices under voltage clamp conditions, and the cell morphology was examined using Lucifer yellow fluorescence with confocal microscopy. The current–voltage relations of the lePSCs in all three types of ganglion cells are approximately linear within the cells' physiological range. The average chloride/cation conductance ratio ($\Delta g_{Cl}(NR)/\Delta g_C(NR)$) of the lePSCs is near 3, suggesting that ganglion cell light responses are associated with a greater postsynaptic conductance change at the amacrine-ganglion cell inhibitory synapses than at the bipolar-ganglion cell excitatory synapses. By comparing the charge transfer of lePSCs in normal Ringer's and in picrotoxin + strychnine + Imidazole-4-acidic acid, we found that the GABAergic and glycinergic amacrine–bipolar cell feedback synapses decreased the light-induced glutamatergic vesicle release from bipolar cells to all ganglion cells, and the degree of release reduction varied widely from ganglion cell to ganglion cell, with a range of 3–28 fold. © 2002 Elsevier Science Ltd. All rights reserved.

Keywords: Light-evoked postsynaptic currents; Dendritic stratification; Cation conductance; Chloride conductance; Confocal microscopy; Picrotoxin; Strychnine; Imidazole-4-acidic acid I4AA

1. Introduction

Ganglion cells are the output neurons of the retina. The dendrites of ganglion cells, located in the inner plexiform layer (IPL), receive excitatory synaptic inputs from bipolar cells and inhibitory synaptic inputs from amacrine cells (Werblin & Dowling, 1969). Bipolar cells use glutamate as their neurotransmitter, and it gates a cation conductance with a reversal potential near 0 mV (Belgum, Dvorak, & McReynolds, 1982; Gao & Wu, 1999; Mittman, Taylor, & Copenhagen, 1990). The vast majority of amacrine cells use GABA or glycine as their neurotransmitter (Yang & Yazulla, 1988a,b), which gates chloride conductance with a reversal potential near −60 mV (Mittman et al., 1990; Gao & Wu, 1998). To a steady step of light, ganglion cells give rise to three types of responses: one with an increase of spike activity at the onset of the light step (ON cells), the second with a spike increase at the light offset (OFF cells), and the third exhibiting spike activity at both light onset and offset (ON–OFF cells) (Hensley, Yang, & Wu, 1993; Miller, 1979; Werblin & Dowling, 1969). It is not clear what the relative contributions of the cation and chloride conductance changes are to the light-evoked signals in various types of ganglion cells, or whether the relative strengths of the bipolar/amacrine cell inputs differ for ON and OFF responses.

The light responses of the ON ganglion cells and the ON responses of the ON–OFF ganglion cells are driven by the depolarizing (on-center) bipolar cells (DBCs), and those of the OFF cells and the OFF responses of the ON–OFF cells are driven by the hyperpolarizing (off-center) bipolar cells (HBCs) (Miller, 1979; Werblin & Dowling, 1969). DBCs make synaptic contacts with ganglion cell dendrites predominantly in sublamina B of the IPL, whereas HBCs make synapses with ganglion cell dendrites mainly in sublamina A of the IPL (Famiglietti & Kolb, 1976; Nelson, Famiglietti, & Kolb, 1978; Famiglietti, Kaneko, & Tachibana, 1977; Wu, Gao, & Maple, 2000). Amacrine cells make inhibitory synapses on ganglion cell dendrites (feedforward synapses), on bipolar cell axon terminals that are presynaptic to

* Corresponding author. Tel.: +1-713-798-5966; fax: +1-713-798-6457.
E-mail address: swu@bcm.tmc.edu (S.M. Wu).

0042-6989/02/$ - see front matter
PII: S0042-6989(01)00258-9

ganglion cells (feedback synapses), and on other amacrine cells (Wong-Riley, 1974; Muller & Marc, 1990; Marc & Liu, 2000). The GABAergic feedforward synapses are mediated largely by $GABA_A$ receptors on ganglion cells and the GABAergic feedback synapses are mainly mediated by $GABA_C$ receptors on bipolar cell axon terminals (Lukasiewicz & Shields, 1998; Gao, Maple, & Wu, 2000). Glycinergic feedforward and feedback synapses are mediated by strychnine-sensitive glycine receptors (Maple & Wu, 1998). It is not clear how the feedback and feedforward synapses modulate light-evoked signals or what the relative contributions of these two synapses are to the light-evoked conductance changes in retinal ganglion cells.

In this study, we examine the light-evoked postsynaptic currents (lePSCs) under voltage clamp conditions from salamander ON, OFF and ON–OFF ganglion cells in the absence and presence of picrotoxin, imidazole-4-acidic acid (I4AA) and strychnine, which block the $GABA_A$, $GABA_C$ and glycine receptors in the feedback and feedforward synapses (Gao et al., 2000; Lukasiewicz & Shields, 1998; Maple & Wu, 1998; Muller & Marc, 1990). We measure the current–voltage relations and conductance changes associated with bipolar cell and amacrine cell inputs, and estimate the number of excitatory and inhibitory synaptic vesicles released at light onset and offset in the ON, OFF and ON–OFF ganglion cells.

2. Materials and methods

Larval tiger salamanders (*Ambystoma tigrinum*) purchased from Charles D. Sullivan, Co. (Nashville, TN) and KON's Scientific Co. Inc. (Germantown, WI) were used in this study. The procedures of dissection, retinal slicing and recording were described in previous publications (Werblin, 1978; Wu, 1987). Dissection and recording were done under infrared illumination with a dual-unit FIND-R-SCOPE (FJW Industry, Mount Prospect, IL) and the Nitemare infrared scopes (Meyers and Co. Inc. Redmond, WA). Oxygenated Ringer's solution was introduced continuously to the superfusion chamber, and the control Ringer's contained 108 mM NaCl, 2.5 mM KCl, 1.2 mM $MgCl_2$, 2 mM $CaCl_2$, 5 mM Hepes (adjusted at pH 7.7). All chemicals were dissolved in control Ringer's solution. A photostimulator was used to deliver light spots of 600–1200 μm in diameter to the retina via the epi-illuminator of the microscope. The intensity of unattenuated ($\log I = 0$) 500 nm light was 2.05×10^7 photons $\mu m^{-2}\,s^{-1}$.

Voltage-clamp recordings were made with an Axopatch 200A amplifier connected to a DigiData 1200 interface and pClamp 6.1 software (Axon Instruments, Foster City, CA). Patch electrodes of 5 MΩ tip resistance when filled with internal solution containing 118 mM Cs methanesulfonate, 12 mM CsCl, 5 mM EGTA, 0.5 mM $CaCl_2$, 4 mM ATP, 0.3 mM GTP, 10 mM Tris, 0.8 mM Lucifer yellow, adjusted to pH 7.2 with CsOH were made with Narishige or Sutter patch electrode pullers. All chemicals were obtained from Research Biochemical International (Natick, MA) or Sigma (St Louis, MO), Picrotoxin, I4AA and strychnine solutions were freshly made each time. The chloride equilibrium potential, E_{Cl}, with this internal solution was about −60 mV. Estimates of the liquid junction potential at the tip of the patch electrode prior to seal formation varied from −9.2 to −9.6 mV. For simplicity, we corrected all holding potentials by 10 mV.

Three-dimensional cell morphology was visualized through the use of Lucifer yellow fluorescence with a confocal microscope (Zeiss 510). Images were acquired with a ×40 water immersion objective (n.a. = 0.75), using the 458 nm excitation line of an argon laser, and a long pass 505 nm emission filter. Consecutive optical sections were superimposed to form a single image using the Zeiss LSM-PC software, and these compressed image stacks were further processed in Adobe Photoshop 6.0 to improve the signal to noise ratio. Since signal intensity values were typically enhanced during processing to improve visibility of smaller processes, the cell bodies and larger processes of some cells appear saturated due to their larger volume of fluorophore. Although the background images of the retinal slices were acquired simultaneously with the fluorescent cells, they were imaged using transmitted light. We targeted cells in the ganglion cell layer with somas situated beneath the surface of the slice, and they usually had relatively intact processes (assessed by rotation of the stacked images). In order to avoid displaced amacrine cells, we selected cells that showed a segment of axon attached to the soma. In cases where cells did not show clear axons, the data was discarded.

3. Results

3.1. Light-evoked postsynaptic currents of the ON, OFF and ON–OFF ganglion cells in the presence and absence of GABAergic and glycinergic inhibition

In the tiger salamander retina, about 80% of ganglion cells are ON–OFF cells, 15% are ON cells and only about 5% are OFF cells (Hensley et al., 1993). Fig. 1A shows current traces of an ON (a), an OFF (b) and an ON–OFF (c) ganglion cell recorded under voltage clamp conditions in dark-adapted tiger salamander retinal slices. The zero-current potentials of these cells in darkness were −65, −66 and −62 mV, respectively. We also measured the zero-current potential of 39 other ganglion cells in darkness, and it varied between −55 and −71 mV. Currents were recorded at eight holding

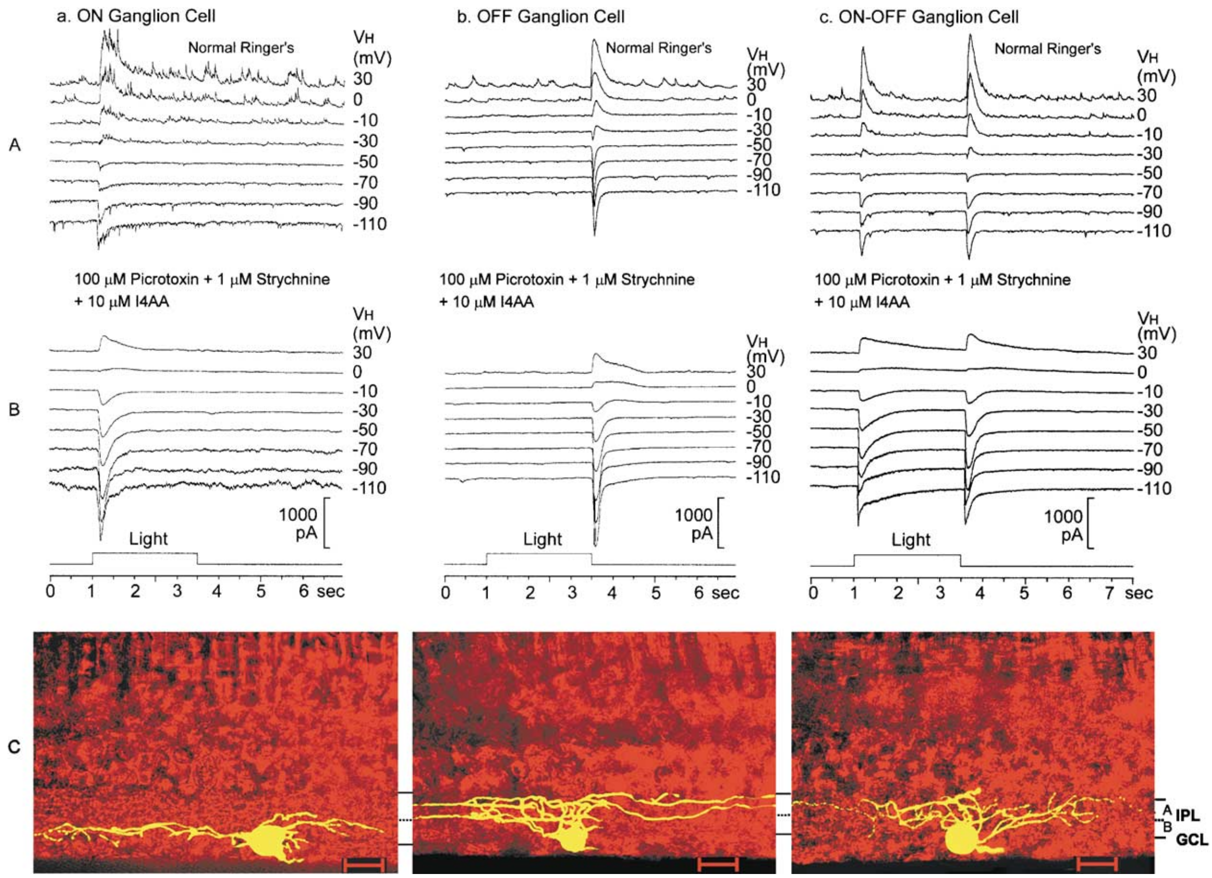

Fig. 1. Current traces of an ON (a), an OFF (b) and an ON–OFF (c) ganglion cell in normal Ringer's (NR) (A), and in the presence of 100 μM picrotoxin, 1 μM strychnine and 10 μM I4AA (P + S + I) (B). Currents were recorded under voltage clamp conditions at eight holding potentials (from −110 to 30 mV with 20 mV increments), and a 2.5 s light step (500 nm, −2 log unit attenuation) was delivered to the cell at each holding potential. Recombined stacks of confocal fluorescent images of the three ganglion cells filled with Lucifer yellow are shown in (C). Images were processed with the Zeiss LSM-PC software and Adobe Photoshop 6.0. The scale bars are 25 μm.

potentials (from −110 to 30 mV with 20 mV increment), and a 2.5 s light step (500 nm, −2 log unit attenuation) was delivered to the cell at each holding potential. LePSCs were observed at stimulus onset of the ON and ON–OFF cells, and at the offset of the stimulus for the OFF and ON–OFF cells. The time course of decay for the transient responses varied from cell to cell (the time from peak to baseline varied between 0.2 and 6 s). The morphology of the three ganglion cells in Fig. 1A was revealed by Lucifer yellow fluorescence with confocal microscopy (Fig. 1C). The ON cell had dendrites that ramified in sublamina B, the OFF cell dendrites ramified in sublamina A, and the ON–OFF cell ramified in both sublamina A and B.

The apparent reversal potential (V_{Rev}) of the lePSCs was between −20 and −50 mV. Since tiger salamander retinal ganglion cells receive glutamatergic excitatory synaptic inputs (with a reversal potential near 0 mV) from bipolar cells, and GABAergic and glycinergic inhibitory synaptic inputs (with a reversal potential near $E_{Cl} = -60$ mV) from amacrine cells (Belgum et al., 1982; Belgum, Dvorak, & McReynolds, 1984; Mittman et al., 1990; Frumkes, Miller, Slaughter, & Dacheux, 1981), the lePSCs with V_{Rev} between −60 and 0 mV are likely to be mediated by a mixture of bipolar cell and amacrine cell inputs. Fig. 1B shows the current responses of the same three ganglion cells shown in Fig. 1A in the presence of 100 μM picrotoxin, 1 μM strychnine and 10 μM I4AA (P + S + I). We used these three compounds to suppress $GABA_A$, glycine and $GABA_C$ receptors in ganglion cells and bipolar cell axon terminals, so that the feedforward and feedback inhibitions from amacrine cells were largely curtailed (Gao et al., 2000; Lukasiewicz & Shields, 1998). In addition to the lePSCs, there were also discrete spontaneous postsynaptic currents (sPSCs), mediated by single or multiples of glutamatergic, GABAergic and glycinergic synaptic vesicle release (Taylor et al., 1995; Gao & Wu, 1998, 1999). The current traces in P + S + I were smoother, because GABAergic and glycinergic spontaneous inhibitory postsynaptic currents (sIPSCs) were blocked (Gao & Wu, 1999). The lePSCs in P + S + I reversed between −10 and 10 mV, consistent with the idea that P + S + I suppresses the inhibitory lePSCs mediated by

GABAergic and glycinergic amacrine cells, and that the residual lePSCs are mediated by bipolar cells through glutamate-gated cation conductances (with a reversal potential ranging from −10 to +10 mV) (Diamond & Copenhagen, 1995; Mittman et al., 1990; Gao & Wu, 1999). By comparing the lePSCs at $E_{Cl} = -60$ mV with and without P + S + I, it is evident that the excitatory light-evoked inputs from bipolar cells are larger and more prolonged when amacrine cell inputs are blocked. This is consistent with the idea that GABAergic and glycinergic amacrine cells not only directly activate chloride conductances in ganglion cells, but also decrease and shorten the output signals of the bipolar cells through the feedback synapses made on bipolar cell axon terminals (Lukasiewicz, Maple, & Werblin, 1994; Dong & Werblin, 1998).

3.2. Current–voltage relations of light-evoked postsynaptic currents and conductance changes mediated by excitatory and inhibitory synaptic inputs

The current–voltage relations of the peak lePSCs of the three ganglion cells shown in Fig. 1 were plotted in Fig. 2. The *I–V* relations in either NR or in P + S + I were approximately linear between 30 and −70 mV (fitted by solid lines), and they were sublinear at voltages below −70 mV (possibly due to the voltage-dependent divalent block of the NMDA receptor-mediated current (Mittman et al., 1990)). The linear portion of the *I–V* relations covers the physiological range of the ON–OFF ganglion cells, because the dark membrane potential of these cells varies from −40 to −70 mV (Belgum et al., 1984; Belgum et al., 1982), and the light-evoked voltage

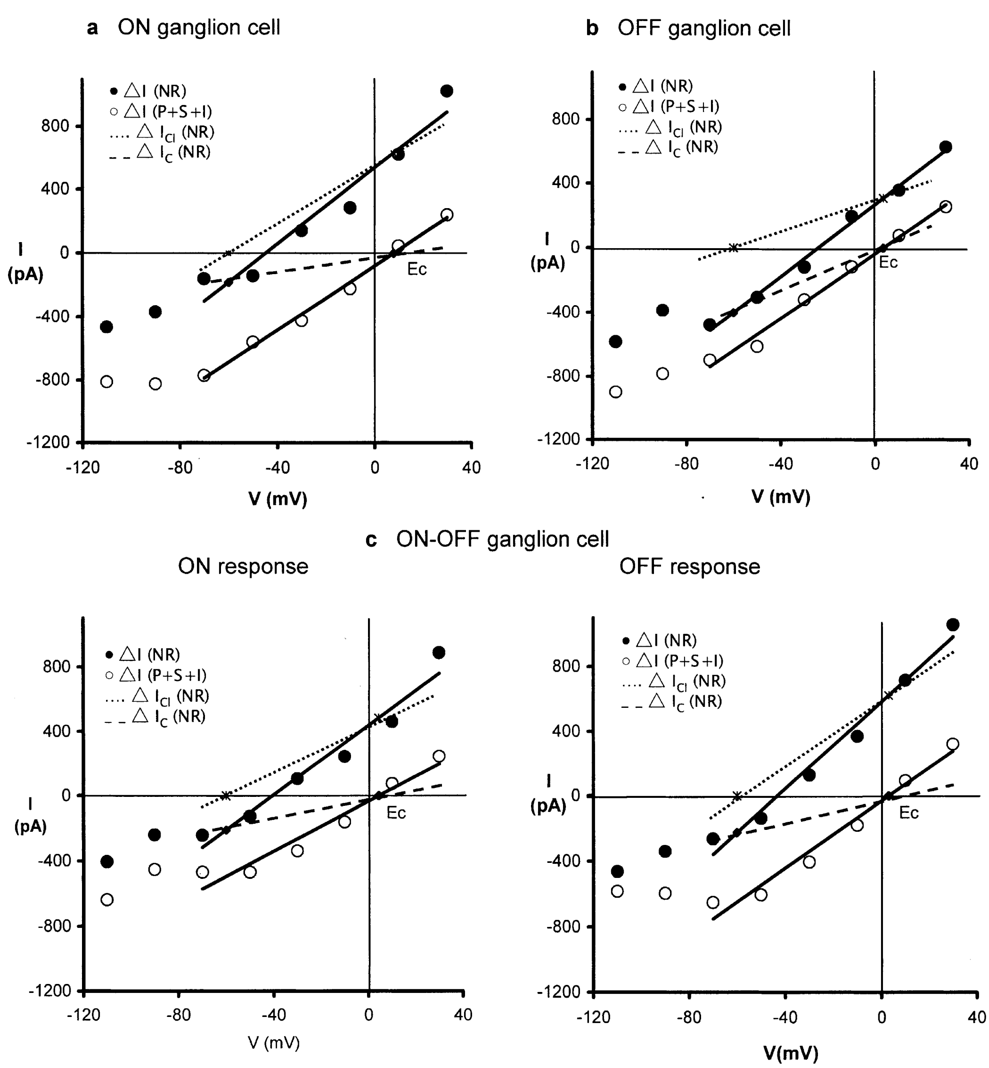

Fig. 2. Current–voltage relations of the peak lePSCs of the three ganglion cells shown in Fig. 1. (a) ON cell, (b) OFF cell and (c) ON–OFF cell. The *I–V* relations in either NR (●) or in P + S + I (○) were approximately linear between 30 mV and −70 mV (fitted by solid lines), and they became sublinear at more negative potentials. Δg_C(NR) and Δg_{Cl}(NR) were determined by Eqs. (1) and (2) and the values are plotted as dashed and dotted lines, respectively. The cation equilibrium potential, E_C, equals to V_{Rev}(P + S + I), and the chloride equilibrium potential, E_{Cl}, was calculated by the Nernst equation to be −60 mV.

responses are depolarizing. For the ON cell (Fig. 2a), the linear I–V relation had a slope in NR (conductance change, $\Delta g_{\mathrm{Total}}$ (NR)) of 11.94 nS, and a slope of 10.10 nS in P + S + I. For the OFF cell (Fig. 2b), the linear I–V slope was 11.21 nS in NR, and 10.07 nS in P + S + I. For the ON–OFF cell (Fig. 2c), the linear I–V slope was 10.78 nS in NR, and 7.68 nS in P + S + I for the ON response, and 13.44 nS in NR, and 10.25 nS in P + S + I for the OFF response.

Since lePSCs in NR are mediated by mixtures of bipolar cell and amacrine cell inputs, the slope of the I–V relations ($\Delta g_{\mathrm{Total}}$) should be equal to the sum of the glutamate-gated cation conductance change (Δg_{C}) and the GABA- and glycine-gated chloride conductance change (Δg_{Cl}). Therefore,

$$\Delta g_{\mathrm{Total}}(\mathrm{NR}) = \Delta g_{\mathrm{C}}(\mathrm{NR}) + \Delta g_{\mathrm{Cl}}(\mathrm{NR}) \tag{1}$$

The apparent reversal potential of lePSCs in NR (V_{Rev} (NR)) is related to the equilibrium potentials of the cation channels (E_{C}) and chloride channels (E_{Cl}) by the following equation (Brown, Muller, & Murray, 1971):

$$V_{\mathrm{Rev}}(\mathrm{NR}) = (\Delta g_{\mathrm{C}}(\mathrm{NR})E_{\mathrm{C}} + \Delta g_{\mathrm{Cl}}(\mathrm{NR})E_{\mathrm{Cl}})/(\Delta g_{\mathrm{C}}(\mathrm{NR}) + \Delta g_{\mathrm{Cl}}(\mathrm{NR})).$$

By rearranging the terms, one obtains:

$$\Delta g_{\mathrm{C}}(\mathrm{NR})/\Delta g_{\mathrm{Cl}}(\mathrm{NR}) = (V_{\mathrm{Rev}}(\mathrm{NR}) - E_{\mathrm{Cl}})/(E_{\mathrm{C}} - V_{\mathrm{Rev}}(\mathrm{NR})) \tag{2}$$

In P + S + I, direct GABAergic and glycinergic inputs (feedforward synapses) to ganglion cells were blocked, thus $\Delta g_{\mathrm{Cl}}(\mathrm{P+S+I}) = 0$, and $\Delta g_{\mathrm{Total}}(\mathrm{P+S+I}) = \Delta g_{\mathrm{C}}(\mathrm{P+S+I})$. The reversal potential of lePSCs in P + S + I should be equal to E_{C}, thus $V_{\mathrm{Rev}}(\mathrm{P+S+I}) = E_{\mathrm{C}}$.

From Fig. 2, $V_{\mathrm{Rev}}(\mathrm{NR})$ are −44.81, −24.21, −40.53 and −43.28 mV for the ON–OFF, ON response and OFF response of the ON–OFF cells, respectively. $V_{\mathrm{Rev}}(\mathrm{P+S+I})$ are 7.85, 3.30, 4.31 and 3.07 mV. The reversal potential of the chloride current, E_{Cl}, was calculated by the Nernst equation to be −60 mV (see Section 2). We also confirmed the value of E_{Cl} by measuring the reversal potentials of the GABA- and glycine-induced postsynaptic currents (in cobalt Ringer's), and the results (not shown) showed that E_{Cl} was near −60 mV.

By substituting the values obtained from Fig. 2 into Eqs. (1) and (2), we calculated $\Delta g_{\mathrm{C}}(\mathrm{NR})$, $\Delta g_{\mathrm{Cl}}(\mathrm{NR})$ and $\Delta g_{\mathrm{C}}(\mathrm{P+S+I})$ of the three ganglion cells shown in Fig. 1, and the values are listed in Table 1 (the ON cell is cell 1 in Table 1(A), the OFF cell is cell 1 in Table 1(B), and the ON–OFF cell is cell 2 in Table 1(C)). The calculated $\Delta g_{\mathrm{C}}(\mathrm{NR})$ and $\Delta g_{\mathrm{Cl}}(\mathrm{NR})$ are plotted as dashed and dotted lines in Fig. 2.

We repeated these experiments on four other ON cells, two other OFF cells, and seven other ON–OFF cells, and the values of V_{Rev} and light-evoked conductance changes in NR and in P + S + I for each cell as well as the average values are given in Table 1. In addition to the 16 cells listed in Table 1, we also examined the effects of picrotoxin + I4AA or picrotoxin + strychnine on 31 other ganglion cells (seven ON cells, five OFF cells and 19 ON–OFF cells), and the results were qualitatively similar to those shown in Fig. 1. One exception was that the light-evoked currents near 0 mV were substantially larger than those in the presence of picrotoxin + strychnine + I4AA, indicating that P + I or P + S could not completely block ΔI_{Cl}. For this reason, these 31 cells were not included in Table 1. Although the exact values varied from cell to cell, all three types of ganglion cells exhibited similar light response characteristics in NR and P + S + I exerted similar actions on all ganglion cells. For example, the I–V relations of all ganglion cells between 30 and −70 mV in NR and in P + S + I were approximately linear. The reversal potentials in NR range from −24 to −58 mV, and in P + S + I (E_{C}) range from −8 to 9 mV. Additionally, P + S + I enhanced and broadened the lePSCs near E_{Cl} (−60 mV) in all cells, indicating that the bipolar cell inputs to all three types of ganglion cells are inhibited by the GABAergic and glycinergic *feedback synapses* (since the driving force of the direct (feedforward) amacrine cell inputs at −60 mV is near zero).

The ratio $\Delta g_{\mathrm{Cl}}(\mathrm{NR})/\Delta g_{\mathrm{C}}(\mathrm{NR})$ of all ganglion cells we examined was greater than 1 (except for one OFF cell whose ratio is 0.77), with an average of 2.73 ± 1.42, indicating that the light-evoked responses of most ganglion cells, either at light onset or light offset, are mediated by a greater chloride conductance increase than cation conductance increase. The conductance ratio varies widely from cell to cell (ranging from 0.77 to 6.38), and it does not correlate with either the cell type or receptive field polarity (ON/OFF). These results suggest that the light responses of different ganglion cells are mediated by different strengths of bipolar cell and amacrine cell inputs, and the ratio of amacrine/bipolar cell-induced postsynaptic conductance change varies widely with an average value near 3.

3.3. Light-evoked release of synaptic vesicles from bipolar cells and amacrine cells to ON, OFF, and ON–OFF ganglion cells

Results described in the previous sections indicate that P + S + I increased not only the peak amplitude, but also the duration of the lePSCs in the ON, OFF and ON–OFF ganglion cells. We therefore measured the charge transfer (Q = current × time, obtained by integrating the area under each current response) of the lePSCs (evoked by 2.5 s, 500 nm, −2 light steps) in ganglion cells in NR and in P + S + I. Table 2 lists the charge transfer at E_{Cl} and E_{C} in NR and in P + S + I of

Table 1

Dark potentials, light-induced conductance changes and the ratios of light-induced chloride and cation conductance changes of five ON cells, three OFF cells, and eight ON–OFF cells in NR and in P + S + I. V_{Rev}(NR) and V_{Rev}(P + S + I): apparent reversal potential (in mV) in NR and P + S + I, respectively; Δg(NR), Δg(P + S + I), Δg_C(NR) and Δg_{Cl}(NR) are light-evoked changes of the cells' total conductance in NR and in P + S + I, cation conductance and chloride conductance (in nS), respectively. Average values ± standard deviation (SD) are given below each set of data

Cell number	V_{Rev}(NR), mV	V_{Rev}(P + S + I), mV	Δg(NR), nS	Δg(P + S + I), nS	Δg_C(NR), nS	Δg_{Cl}(NR), nS	$\Delta g_{Cl}/\Delta g_C$(NR)
A. ON ganglion cells							
1	−44.81	7.85	11.94	10.01	2.68	9.26	3.46
2	−40.38	8.77	14.32	11.59	3.22	11.10	3.45
3	−37.50	−3.11	9.80	10.81	4.21	5.59	1.33
4	−55.22	−7.25	12.14	8.43	3.33	8.81	2.65
5	−33.72	1.37	8.75	11.32	2.70	6.05	2.24
Average	−42.326	1.526	11.390	10.432	3.23	8.162	2.626
±SD	±7.397	±6.181	±1.947	±1.137	±0.557	±2.066	±0.895
B. OFF ganglion cells							
1	−24.21	3.30	11.21	10.07	6.34	4.87	0.77
2	−43.32	5.63	9.32	7.56	4.02	8.30	2.06
3	−39.41	4.33	12.54	13.32	2.88	11.66	4.05
Average	−35.647	4.420	11.023	10.317	4.413	8.277	2.293
±SD	±8.243	±0.953	±1.321	±2.358	±1.439	±2.772	±1.652

Cell number	V_{Rev}(NR), mV		V_{Rev}(P + S + I), mV		Δg(NR), nS		Δg(P + S + I), nS		Δg_C(NR), nS		Δg_{Cl}(NR), nS		$\Delta g_{Cl}/\Delta g_C$(NR)	
C. ON–OFF ganglion cells	ON	OFF	ON	OFF	ON	OFF	ON	OFF	ON	OFF	ON	OFF	ON	OFF
1	−37.52	−44.64	8.04	8.47	7.88	7.18	9.31	9.86	2.61	1.61	5.28	5.57	2.02	3.46
2	−40.53	−43.28	4.31	3.07	10.78	13.44	7.68	10.25	3.26	3.56	7.52	9.88	2.31	2.77
3	−39.62	−45.61	−6.62	−8.31	19.20	10.13	14.10	13.29	7.33	2.81	11.87	7.31	1.62	2.60
4	−50.34	−51.28	−1.93	−4.41	14.18	13.29	8.63	4.98	2.36	4.98	11.82	11.21	5.01	2.25
5	−41.02	−41.75	−1.29	−2.26	7.22	6.94	8.72	7.59	2.33	2.19	4.98	4.75	2.10	2.17
6	−57.90	−50.20	−1.50	−4.92	7.24	5.64	7.60	7.01	1.03	1.01	6.57	6.00	6.38	5.94
7	−43.40	−41.30	1.76	2.33	8.75	8.28	9.02	8.88	3.08	2.72	5.67	5.56	1.84	2.04
8	−37.20	−39.40	1.37	4.08	8.15	12.00	11.12	13.20	2.77	5.88	5.38	6.12	1.94	1.04
Average	−43.440	−44.680	0.518	−0.244	10.430	9.613	9.523	9.383	3.096	3.095	7.363	7.050	2.903	2.780
±SD	±6.700	±3.950	±4.146	±5.251	±3.970	±2.845	±2.010	±2.723	±1.721	±1.546	±2.703	±2.152	±1.773	±1.450

Table 2
Light-induced charge transfer and the ratios of charge transfer at E_{Cl} and E_C in NR and in P + S + I of the same 16 ganglion cells listed in Table 1. Q_C and Q_{Cl} are light-evoked cation and chloride charge transfers (in pC). Average values ± standard deviation (SD) are given below each set of data

Cell number	NR				P + S + I		$Q_C(P+S+I)/Q_C(NR)$	
	Q_C, pC		Q_{Cl}, pC		Q_C, pC			
A. ON ganglion cells								
1	−62		287		−206		3.3	
2	−103		328		−432		4.2	
3	−19		138		−340		17.9	
4	−18		125		−224		12.4	
5	−39		185		−186		4.8	
Average	−48.2		212.6		−277.6		8.88	
±SD	±31.8		±81.1		±93.9		±7.056	
B. OFF ganglion cells								
1	−43		65		−149		3.5	
2	−61		201		−240		3.9	
3	−35		112		−282		8.1	
Average	−46.3		126		−223		5.167	
±SD	±10.80		±56.4		±55.5		±2.548	
C. ON–OFF ganglion cells								
	ON	OFF	ON	OFF	ON	OFF	ON	OFF
1	−8	−7	125	87	−224	−134	28.0	19.1
2	−35	−43	115	135	−209	−164	5.9	3.8
3	−137	−35	326	123	−183	−95	1.3	2.7
4	−20	−24	193	160	−267	−58	13.4	2.4
5	−17	−10	125	83	−162	−74	9.5	7.4
6	−45	−54	187	242	−245	−312	5.4	5.8
7	−11	−23	135	185	−198	−294	18.0	12.8
8	−27	−20	145	103	−222	−114	8.2	5.7
Average	−37.5	27.0	172.6	139.8	−213.8	−155.6	11.21	7.46
±SD	±39.3	±15.0	±74.4	±50.7	±31.4	±90.7	±8.49	±5.75

the five ON cells, three OFF cells and eight ON–OFF cells listed in Table 1. At E_{Cl} (−60 mV), where the chloride charge transfer was near zero, Q was carried almost completely by cation charge transfer (Q_C) at the glutamatergic synapses, and at E_C (0 mV), where the cation charge transfer was near zero, Q was carried almost completely by chloride charge transfer (Q_{Cl}) at the GABAergic and glycinergic synapses. The ratio $Q_C(P+S+I)/Q_C(NR)$ gives the relative cation charge transfer mediated by bipolar cell inputs in the absence and presence of feedback synapses.

Anatomical and physiological evidence has suggested that bipolar cells communicate with ganglion cells via vesicular chemical synapses (Wong-Riley, 1974; Von Gersdorff & Matthews, 1994). From an earlier study, the charge transfer mediated by glutamate released from a single vesicle (q) at the bipolar-ganglion cell synapses (holding potential = −60 mV) is about −0.0355 pC (Gao & Wu, 1999), which is close to the result of a similar study (Taylor et al., 1995). Therefore the number of glutamatergic synaptic vesicles released by light from bipolar cells to ganglion cells can be estimated by the ratio of light-induced charge transfer to the charge transfer of a single vesicle (Q_C/q). From the Q_C values given in Table 2, we were able to estimate that a 2.5 s, 500 nm, −2 light step on average evoked a release of 1358 (48.2/0.0355) glutamatergic synaptic vesicles from bipolar cells to an ON cell, 1304 (46.3/0.0355) vesicles to an OFF cell, 1056 (37.5/0.0355) vesicles to a ON–OFF ganglion cell at the light onset, and 761 (27/0.0355) vesicles at the light offset. In the presence of P + S + I while feedback synapses were blocked, the same light step evoked a release of 7820 (277.6/0.0355) glutamatergic synaptic vesicles from bipolar cells to an ON cell, 6282 (233/0.0355) vesicles to an OFF cell, 6023 (213.8/0.0355) vesicles to an ON–OFF ganglion cell at light onset, and 4383 (155.6/0.0355) vesicles at light offset. These results suggest that the number of glutamatergic synaptic vesicles released by the light step in the absence of presynaptic inhibition was 5.76 (7820/1358) fold higher than the number of vesicles released in the presence of presynaptic inhibition for the ON cells, 4.82 (6282/1304) fold higher for OFF cells, and 5.70 (6023/1056) fold higher at light onset and 5.76 (4383/761) fold higher at light offset for ON–OFF cells.

By using the same scheme, we estimated the number of GABAergic/glycinergic vesicles released from amacrine cells to ganglion cells (feedforward synapses). At

E_C (list in Table 1 for each cell), where the cation charge transfer was near zero, the average Q in NR, carried almost completely by chloride ions, was 212.6 pC in the ON cells, 126 pC in the OFF cells, 172.6 pC at the light onset, and 139.8 pC at the light offset in the ON–OFF cells (Table 2). From an earlier study, the charge transfer mediated by GABA or glycine released from a single vesicle near 0 mV is about 1.06 pC (Gao & Wu, 1998). Therefore in NR, a 2.5 s, 500 nm, −2 light step on average released 201 (212.6/1.06) GABAergic/glycinergic synaptic vesicles from amacrine cells to an ON cell, 119 (126/1.06) vesicles to an OFF cell, 163 (172.6/1.06) vesicles at the light onset and 132 (139.8/1.06) vesicles at the light offset to an ON–OFF cell.

4. Discussion

Our results suggest the current–voltage relations of the lePSCs in all three types of ganglion cells (ON, OFF and ON–OFF cells) are approximately linear within the cells' physiological range (between −70 and 30 mV). It has been shown that the excitatory lePSCs of salamander ganglion cells have two components: an AMPA receptor-mediated "early" component and a NMDA receptor-mediated "late" component (Mittman et al., 1990). Since our *I–V* relations were obtained by plotting the early current peaks, they largely reflect the early AMPA component which is approximately linear (Lukasiewicz, Wilson, & Lawrence, 1997). The "late" non-linear NMDA component only slightly influences the peak currents at potentials above −70 mV, but its contribution (reduces peak currents to sublinear values) becomes more significant at potentials below −70 mV because the divalent block on NMDA receptors is stronger at more negative potentials (Nowak, Bregestovski, Ascher, Herbet, & Prochiantz, 1984).

Based on the linear *I–V* relations at potentials above −70 mV, we were able to estimate the postsynaptic conductance changes associated with light-evoked cation currents and chloride currents mediated by the glutamatergic and GABAergic/glycinergic synapses. It is worth noting that our data only show $\Delta I(\mathrm{NR}) = \Delta I_C + \Delta I_{Cl}$ is approximately linear, which does not necessarily mean that $\Delta I_C(\mathrm{NR})$ and $\Delta I_{Cl}(\mathrm{NR})$ are linear. However, we think that $\Delta I_C(\mathrm{NR})$ and $\Delta I_{Cl}(\mathrm{NR})$ are linear between −70 and +30 mV for two reasons. First, the *I–V* relations of the AMPA-, GABA- and glycine-induced currents in ganglion cells are approximately linear within this potential range (Lukasiewicz & McReynolds, 1985; Belgum et al., 1982, 1984; Lukasiewicz & Werblin, 1990; Lukasiewicz et al., 1997). Secondly, the cation current in P + S + I ($\Delta I_C(\mathrm{P+S+I})$) is linear between −70 and +30 mV (Fig. 2), and thus the cation current in NR ($\Delta I_C(\mathrm{NR})$) is likely to be linear. Therefore $\Delta I_{Cl}(\mathrm{NR})$ is linear because $\Delta I(\mathrm{NR}) = \Delta I_C + \Delta I_{Cl}$ is linear.

In Table 1, we show that the average chloride/cation conductance ratio ($\Delta g_{Cl}(\mathrm{NR})/\Delta g_C(\mathrm{NR})$) of the lePSCs is near 3 for all three types of ganglion cells. This suggests that in almost all ganglion cells, light elicits a greater total postsynaptic conductance change at the amacrine-ganglion cell inhibitory synapses than at the bipolar-ganglion cell excitatory synapses. However, since the dark membrane potentials of ganglion cells (−55 to −71 mV, see above) are much closer to E_{Cl} (−60 mV) than to E_C (between −10 and 10 mV, see above), the amacrine cell-mediated inhibitory *voltage* response may not be as large as the bipolar cell-mediated excitatory *voltage* response. The GABAergic and glycinergic feedforward synapses inhibit the excitatory bipolar cell inputs largely by voltage shunting.

At −60 mV where the feedforward inhibitory inputs are near zero, P + S + I enhances and prolongs the light-evoked excitatory responses in all three types of ganglion cells. This result suggests that the GABAergic and glycinergic inhibitory synapses on bipolar cells (feedback synapses) reduce and shorten the light-evoked excitatory signals from bipolar cells to ganglion cells. In Table 2, we list the ratio $Q_C(\mathrm{P+S+I})/Q_C(\mathrm{NR})$ of individual ganglion cells, and from the value of charge transfer for single glutamatergic vesicles (Taylor et al., 1995; Gao & Wu, 1999), we estimated the number of vesicles released by light in the absence and presence of feedback synapses. Our data show that the feedback synapses reduce the glutamatergic vesicle release from bipolar cells to different ganglion cells by various degrees, ranging from 3 to 28 fold.

A previous report has shown that the amplitudes of lePSCs in salamander ON–OFF ganglion cells are *reduced* by bicuculline and strychnine (Mittman et al., 1990). This differs from our results in which picrotoxin, I4AA and strychnine enhance and prolong the lePSCs. Bicuculline is known to be a $\mathrm{GABA_A}$ receptor antagonist, but not a $\mathrm{GABA_C}$ receptor antagonist, whereas picrotoxin and I4AA block both $\mathrm{GABA_A}$ and $\mathrm{GABA_C}$ receptors (Qian & Dowling, 1993, 1994). Since GABA responses in ganglion cells are largely mediated by $\mathrm{GABA_A}$ receptors (Lukasiewicz et al., 1994), it is conceivable that bicuculline reduces the lePSCs at potentials away from E_{Cl} by blocking the postsynaptic Δg_{Cl} mediated by the feedfoward synapses. GABA receptors in bipolar cell synaptic terminals are mediated by $\mathrm{GABA_C}$ receptors (Lukasiewicz et al., 1994; Gao et al., 2000), therefore picrotoxin + strychnine + I4AA enhance the lePSCs at potentials near or below E_{Cl} (Fig. 1A) because their presynaptic action (resulting in an increase of light-evoked glutamate release) is more dominant than their postsynaptic actions, due to a larger driving force for the cation current. At potentials near or above E_C, P + S + I reduces lePSCs (Fig. 1A) because their postsynaptic action is more dominant, due to a larger driving force for the chloride current.

Acknowledgements

We thank Drs. Bruce Maple and Roy Jacoby for critically reading this manuscript. This work was supported by grants from NIH (EY 04446, EY 02520), the Retina Research Foundation (Houston), and the Research to Prevent Blindness, Inc.

References

Belgum, J. H., Dvorak, D. R., & McReynolds, J. S. (1982). Sustained synaptic input to ganglion cells of mudpuppy retina. *Journal of Physiology (London)*, *326*, 91–108.

Belgum, J. H., Dvorak, D. R., & McReynolds, J. S. (1984). Strychnine blocks transient but not sustained inhibition in mudpuppy retinal ganglion cells. *Journal of Physiology*, *354*, 273–286.

Brown, J. E., Muller, K. J., & Murray, G. (1971). Reversal potential for an electrophysiological event generated bt conductance changes: a mathematical analysis. *Science*, *174*, 318–320.

Diamond, J. S., & Copenhagen, D. R. (1995). The relationship between light-evoked synaptic excitation and spiking behaviour of salamander retinal ganglion cells. *Journal of Physiology*, *487*, 711–725.

Dong, C. J., & Werblin, F. S. (1998). Temporal contrast enhancement via GABAc feedback at bipolar terminals in the tiger salamander retina. *Journal of Neurophysiology*, *79*, 2171–2180.

Famiglietti, E. V., Jr., Kaneko, A., & Tachibana, M. (1977). Neuronal architecture of on and off pathways to ganglion cells in the carp retina. *Science*, *198*, 1267–1269.

Famiglietti, E. V., Jr., & Kolb, H. (1976). Structural basis for ON- and OFF-center responses in retinal ganglion cells. *Science*, *194*, 193–195.

Frumkes, T. E., Miller, R. F., Slaughter, M., & Dacheux, R. F. (1981). Physiological and pharmacological basis of GABA and glycine action on neurons of mudpuppy retina. III. Amacrine-mediated inhibitory influences on ganglion cell receptive-field organization: a model. *Journal of Neurophysiology*, *45*, 783–804.

Gao, F., Maple, B. R., & Wu, S. M. (2000). An I4AA-sensitive chloride current contributes to the center light responses of bipolar cells in the tiger salamander retina. *Journal of Neurophysiology*, *83*, 3473–3482.

Gao, F., & Wu, S. M. (1998). Characterization of spontaneous inhibitory synaptic currents in salamander retinal ganglion cells. *Journal of Neurophysiology*, *80*, 1752–1764.

Gao, F., & Wu, S. M. (1999). Multiple types of spontaneous excitatory synaptic currents in salamander retinal ganglion cells. *Brain Research*, *21*, 487–502.

Hensley, S. H., Yang, X. L., & Wu, S. M. (1993). Relative contribution of rod and cone inputs to bipolar cells and ganglion cells in the tiger salamander retina. *Journal of Neurophysiology*, *69*, 2086–2098.

Lukasiewicz, P., & Shields, C. R. (1998). Different combinations of GABAa and GABAc receptors confer distinct temporal properties to retinal synaptic responses. *Journal of Neurophysiology*, *79*, 3157–3167.

Lukasiewicz, P. D., Maple, B. R., & Werblin, F. S. (1994). A novel GABA receptor on bipolar cell terminals in the tiger salamander retina. *Journal of Neuroscience*, *14*, 1202–1212.

Lukasiewicz, P. D., & McReynolds, J. S. (1985). Synaptic transmission at N-methyl-D-aspartate receptors in the proximal retina of the mudpuppy. *Journal of Physiology*, *367*, 99–115.

Lukasiewicz, P. D., & Werblin, F. S. (1990). The spatial distribution of excitatory and inhibitory inputs to ganglion cell dendrites in the tiger salamander retina. *Journal of Neuroscience*, *10*, 210–221.

Lukasiewicz, P. D., Wilson, J. A., & Lawrence, J. E. (1997). AMPA-preferring receptors mediate excitatory synaptic inputs to retinal ganglion cells. *Journal of Neurophysiology*, *77*, 57–64.

Maple, B. R., & Wu, S. M. (1998). Glycinergic synaptic inputs to bipolar cells in the tiger salamander retina. *Journal of Physiology*, *506*(3), 731–744.

Marc, R. E., & Liu, W. L. S. (2000). Fundamental GABAergic amacrine cell circuitries in the retina: nested feedback, concatenated inhibition, and axosomatic synapses. *Journal of Comparative Neurology*, *425*, 560–582.

Miller, R. F. (1979). The neuronal basis of ganglion cell receptive field organization and the physiology of amacrine cells. In F. O. Schmidt, F. G. Worden (Eds.), The Neuroscience Fourth Study Program (pp. 227–245), Cambridge, MA: The MIT Press.

Mittman, S., Taylor, W. R., & Copenhagen, D. R. (1990). Concomitant activation of two types of glutamate receptor mediates excitation of salamander retinal ganglion cells. *Journal of Physiology*, *428*, 175–197.

Muller, J. F., & Marc, R. E. (1990). GABAergic and glycinergic pathways in the inner plexiform layer of the goldfish retina. *Journal of Comparative Neurology*, *291*, 281–304.

Nelson, R., Famiglietti, E. V., Jr., & Kolb, H. (1978). Intracellular staining reveals different levels of stratification for on- and off-center ganglion cells in cat retina. *Journal of Neurophysiology*, *41*, 472–483.

Nowak, L., Bregestovski, P., Ascher, A., Herbet, A., & Prochiantz, A. (1984). Magesium gates glutamate activated channels in mouse central neurons. *Nature*, *307*, 462–465.

Qian, H., & Dowling, J. E. (1993). Novel GABA responses from rod-driven retinal horizontal cells. *Nature*, *361*, 162–164.

Qian, H., & Dowling, J. E. (1994). Pharmacology of novel GABA receptors found on rod horizontal cells of the white perch retina. *Journal of Neuroscience*, *14*, 4299–4307.

Taylor, W. R., Chen, E., & Copenhagen, D. R. (1995). Characterization of spontaneous excitatory synaptic currents in salamander retinal ganglion cells. *Journal of Physiology*, *486*(1), 207–221.

Von Gersdorff, H., & Matthews, G. (1994). Dynamics of synaptic vesicle fusion and membrane retrieval in synaptic terminals. *Nature*, *367*, 735–739.

Werblin, F. S. (1978). Transmission along and between rods in the tiger salamander retina. *Journal of Physiology*, *280*, 449–470.

Werblin, F. S., & Dowling, J. E. (1969). Organization of the retina of the mudpuppy, Necturus maculosus. II. Intracellular recording. *Journal of Neurophysiology*, *32*, 339–355.

Wong-Riley, M. T. T. (1974). Synaptic organization of the inner plexiform layer in the retina of the tiger salamander. *Journal of Neurocytology*, *3*, 1–33.

Wu, S. M. (1987). Synaptic connections between neurons in living slices of the larval tiger salamander retina. *Journal of Neuroscience Methods*, *20*, 139–149.

Wu, S. M., Gao, F., & Maple, B. R. (2000). Functional architecture of synapses in the inner retina: segregation of visual signals by stratification of bipolar cell axon terminals. *Journal of Neuroscience*, *20*(2), 4462–4470.

Yang, C. Y., & Yazulla, S. (1988a). Light-microscopic localization of putative glycinergic neurons in the larval tiger slamander retina by immunocytochemical and autoradiographic methods. *Journal of Comparative Neurology*, *272*, 343–357.

Yang, C. Y., & Yazulla, S. (1988b). Localization of putative GABAergic neurons in the larval tiger salamander retina by immunocytochemical and autoradiographic methods. *Journal of Comparative Neurology*, *277*, 96–108.